

Deformation Measurements of Randomly Rough Surfaces

Alexander I. Bennett¹ · Sean Rohde¹ · Kathryn L. Harris² · Kyle D. Schulze¹ ·
Juan Manuel Uruña¹ · Angela A. Pitenis¹ · Peter G. Ifju¹ · Thomas E. Angelini^{1,3} ·
Martin H. Müser⁴ · W. G. Sawyer^{1,2,3}

Received: 13 April 2017 / Accepted: 28 July 2017 / Published online: 22 August 2017
© Springer Science+Business Media, LLC 2017

Abstract Measurements of surface deformations as part of the “Contact Mechanics Challenge” were collected using digital image correlation (DIC). For these experiments, a scaled version (1000×) of the periodic and random roughness surface provided for the “Contact Mechanics Challenge” was used. A 100 mm × 100 mm scale replica of the surface, approximately 10 mm thick, was 3D-printed using an opaque polymethylmethacrylate and pressed into contact against flat, transparent polydimethylsiloxane (PDMS) sheets with dead weight loads. Four different formulations of PDMS were used, and the resulting elastic moduli ranged from 64 kPa to 2.1 MPa. The DIC technique was used in situ to measure the deformation of the PDMS surface at each load increment from 22.5 to 450 N. Surface deformations in and out of contact were measured across the entire apparent area of contact and overlaid with the measurements of contact area to provide a complete description of the surface profile during loading. A direct comparison between these experiments and the simulations regarding the gap within the contact at a reduced pressure

of 0.164 agrees to within ±10% when normalized to the maximum gap.

Keywords Contact Mechanics Challenge · Rough surfaces · Mechanics

1 Introduction

In the “Contact Mechanics Challenge” for the modeling community, there is a statement regarding the complete lack of experimental verification of the models, at least as of 2015 [1, 2]. The motivation of the experimental efforts reported here is focused on trying to fulfill some of the needs from the community. In a previous study by our group, direct measurements of contact area were performed using frustrated total internal reflection (FTIR) to capture the contact locations during a loading with a 100 mm × 100 mm 3D-printed solid replica of the original model surface offered for the Challenge [3]; this represents a scaling of 1000× over the original model. The FTIR experiments measuring relative contact areas, contact distributions, and percolation threshold compared favorably with the simulation results, despite being run on a surface that was scaled by 1000×, non-periodic contact conditions, and having a finite thickness of the deforming elastic surface. The “Contact Mechanics Challenge” had a number of computations requested that were more complex than simple contact area and contact patch distributions. In our experience, the FTIR method was unable to address these questions as the only directly measureable quantities were contact locations.

In order to measure surface deformations, we turned to another optical technique called digital image correlation (DIC). DIC uses a pair of digital cameras to measure the

This article is part of the Topical Collection on Special Issue: The Contact Mechanics Challenge.

✉ W. G. Sawyer
wgsawyer@ufl.edu

¹ Department of Mechanical and Aerospace Engineering, University of Florida, Gainesville, FL 32611, USA

² Department of Materials Science and Engineering, University of Florida, Gainesville, FL 32611, USA

³ Department of Biomedical Engineering, University of Florida, Gainesville, FL 32611, USA

⁴ Department of Materials Science and Engineering, Saarland University, 66123 Saarbrücken, Germany

full-field deformation of an object's surface using stereoscopic method [4–7]. It is a well-established and well-studied technique that requires the surface upon which deformations are to be measured to be completely covered with a random ensemble of black speckles [8, 9]. All of the deformation measurements will be made by tracking the movement of these speckles during loading. The use of a single camera with the DIC method is capable of measuring in-plane deformations on a flat surface. When one camera is used, the 2D images enable in-plane displacements on a flat surface to be measured by performing correlations between the loaded and unloaded images. By extension, when two cameras are used, the pair of images for both the loaded and unloaded conditions enables the measurement of surface deformations in 3D and is not limited by geometry (other than being within the optical path of the cameras). Calibration techniques are used to determine the positions and optical path of the cameras and to compute the uncertainties in the measurements. In these experiments, the DIC measurements compare subset regions in both images and use a cross-correlation function and optimization routines to solve for the displacements.

In this manuscript, we report on the methods and representative results from performing deformation measurements using DIC on scaled experiments to measure the deformations under the contact of randomly rough surfaces. Additionally, we will provide a comparison between the experiments and simulation for the surface gap as defined by the “Contact Mechanics Challenge”; this was not something that could be directly measured, and we used the experiments to find the surface deformations which we subtract from the coordinates of the scaled rough surface along the same line.

2 Experimental Methods and Apparatus

2.1 Sample Preparation

The samples used in this manuscript were the same samples as described by Bennett et al. [3]; briefly, a scaled model of the surface defined by Müser and Dapp [2] was produced using a 3D printing technique. The model surface was scaled globally by a uniform factor of $1000\times$ (i.e., the original $100\ \mu\text{m} \times 100\ \mu\text{m}$ square projection of the surface was fabricated at a size of $100\ \text{mm} \times 100\ \text{mm}$). This 3D-printed solid sample was made from an opaque polymethylmethacrylate (PMMA) print material.

The “Contact Mechanics Challenge” was designed around the numerical challenge of computing the contact and deformation that occurs on a smooth, soft, elastic surface in contact with a rough surface. In the simulation, the contact problem as posed was periodic and semi-

infinite. For these experiments, we produced thin, smooth, flat, and transparent surfaces of polydimethylsiloxane (PDMS), which were made from a two-part curing of Sylgard[®] 184 at four different base/agent ratios (10:1, 20:1, 30:1, and 40:1). These PDMS samples were fabricated into transparent cylindrical sheets ($\sim 15\ \text{mm}$ in thickness) that were bonded onto low-iron glass plates (Starphire[®]), which were $6.35\ \text{mm}$ in thickness.

The elastic modulus of each PDMS sample was measured through in situ optical micro-indentation, and these data are published in the manuscript by Bennett et al. [3]. The modulus, E , and work of adhesion, $\Delta\gamma$, were calculated by fitting the Johnson–Kendall–Roberts (JKR) contact model to the loading curve, which plots the measured contact diameter as a function of the applied load [10]. The results of these experiments for the different formations were: (10:1) $E = 2.1\ \text{MPa}$ $\Delta\gamma = 4\ \text{mJ/m}^2$; (20:1) $E = 0.75\ \text{MPa}$ $\Delta\gamma = 3\ \text{mJ/m}^2$; (30:1) $E = 0.24\ \text{MPa}$ $\Delta\gamma = 2\ \text{mJ/m}^2$; and (40:1) $E = 0.06\ \text{MPa}$ $\Delta\gamma = 3\ \text{mJ/m}^2$. The contribution of adhesion to these contact mechanics experiments is minimal for a number of reasons—the scaling of the model essentially ensures that the effect of adhesion is negligible almost regardless of any adhesion from the PDMS [11, 12], which were found to be small during the monotonic loading curves measured by JKR, and finally all contact experiments were performed by monotonically increasing load, and no unloading measurements were performed. This lack of adhesion in the experimental work is not a major deviation from the simulations, which revealed a minimal contribution from the adhesion in the contact area computations [13].

2.2 Measurements of the Surface Deformation Using Digital Image Correlation (DIC)

As briefly discussed in the Introduction section, DIC is an established measurement technique that is capable of quantitatively measuring deformations in 3D using stereoscopic imaging. The DIC method uses a pair of digital cameras to simultaneously capture a 2D image of a random pattern of surface features (speckles) as they undergo strain and deformation. A schematic of the DIC setup is shown in Fig. 1a, along with the random speckle pattern that was applied to the PDMS surface as shown in Fig. 1b. The black speckles are intentionally randomly shaped with characteristic length scales on the order of $50\text{--}500\ \mu\text{m}$. The random nature of the shape of an individual speckle and the positioning of the speckles relative to one another allow a pair of 2D images to be used to track full-field deformations in 3D [14]. A representative line scan which results from the DIC measurements showing both in-plane and out-of-plane deformations and an

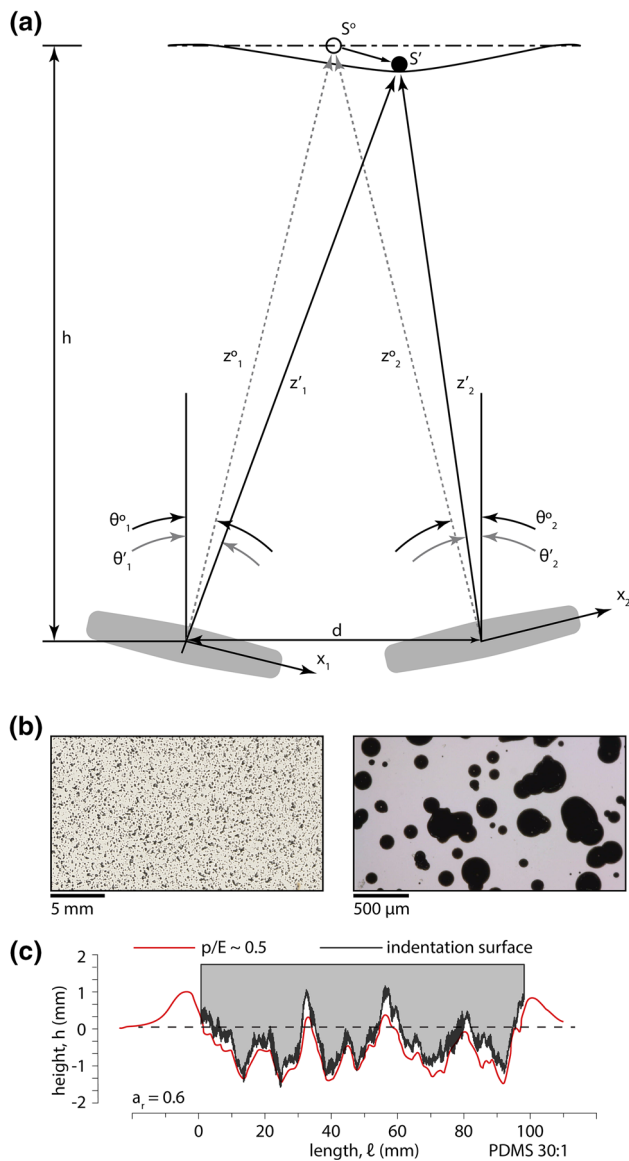


Fig. 1 Digital Image Correlation. **a** Stereoscopic placement of cameras focused on top surface of PDMS sample. **b** Speckle pattern at $\times 1$ (left) and $\times 240$ (right). **c** Line scan of deformation data for 30:1 PDMS at $x = 50$ mm and 0 mm $< y < 100$ mm

associated line scan through the model surface is shown in Fig. 1c.

2.3 Experimental Procedure

The scaled 3D-printed surface was placed into contact with the speckled surface of the PDMS without any applied load, and the loading procedure used specific increments of 4.5 N until 45 N was achieved, and then 22.5 N increments until 450 N was achieved. These loads were applied by gently placing weights onto the flat back surface of the 3D-printed model. The loading was performed using a quasi-

static method and a sequential method, where the DIC images were taken at each load. The time between the loading of the contact and imaging varied but was generally under 100 s. Over this time period, the measurements of contact area did not noticeably vary for the four PDMS samples used, although this was not a parameter that was investigated. The manual loading method was identical to the approach described by Bennett et al. [3].

3 Results and Discussion

The 3D deformation field of the PDMS samples is shown for the four different samples, at five different loads (from 22.5 to 450 N) in Fig. 2. The maximum deformation was on the order of 2.5 mm and was found on the softest PDMS sample at the highest load. Considering that the PDMS thickness was only 15 mm, this represents a significant strain and a considerable difference between the setup of the simulations and these experiments. A full 3D deformation field was not part of the ‘‘Contact Mechanics Challenge,’’ and therefore a direct comparison is not available, but the patterns in the graphs are striking. As the reduced pressure increases, so too do the overall area and magnitude of deformation, along with the maximum depth of penetration. One of the most intriguing results from these measurements is the degree of negative deformation, which in these measurements represents a surface feature moving up (i.e., the opposite direction from the indentation motion). In Fig. 1c, the deformation along the centerline is shown at a reduced pressure of 0.5. It is readily apparent that the deformation at the edge of contact is negative and roughly symmetric, which is not the expected profile for a punch against a semi-infinite half-space [15]. This deformation profile is a result of the finite thickness of the elastomer sample and suggests that comparisons between these experiments and simulations may not be appropriate. However, the simulations have a computationally efficient and elegant approach that uses a periodic indentation surface (i.e., there is no edge of contact) for the elastic half-space. Therefore, as a most simple possible explanation, conservation rules predict that both the experimental approach and the numerical simulations will produce both positive and negative deformation within the contacts.

A combined image of contact area and deformation (mm) at a reduced pressure of 0.16 and a relative contact area that was just beyond the percolation threshold is shown in Fig. 3a. This plot was made by overlaying the contact area measurements obtained by using the FTIR technique by Bennett et al. [3] at the same experimental conditions (the data sets were aligned using the largest peaks as intrinsic fiducials).

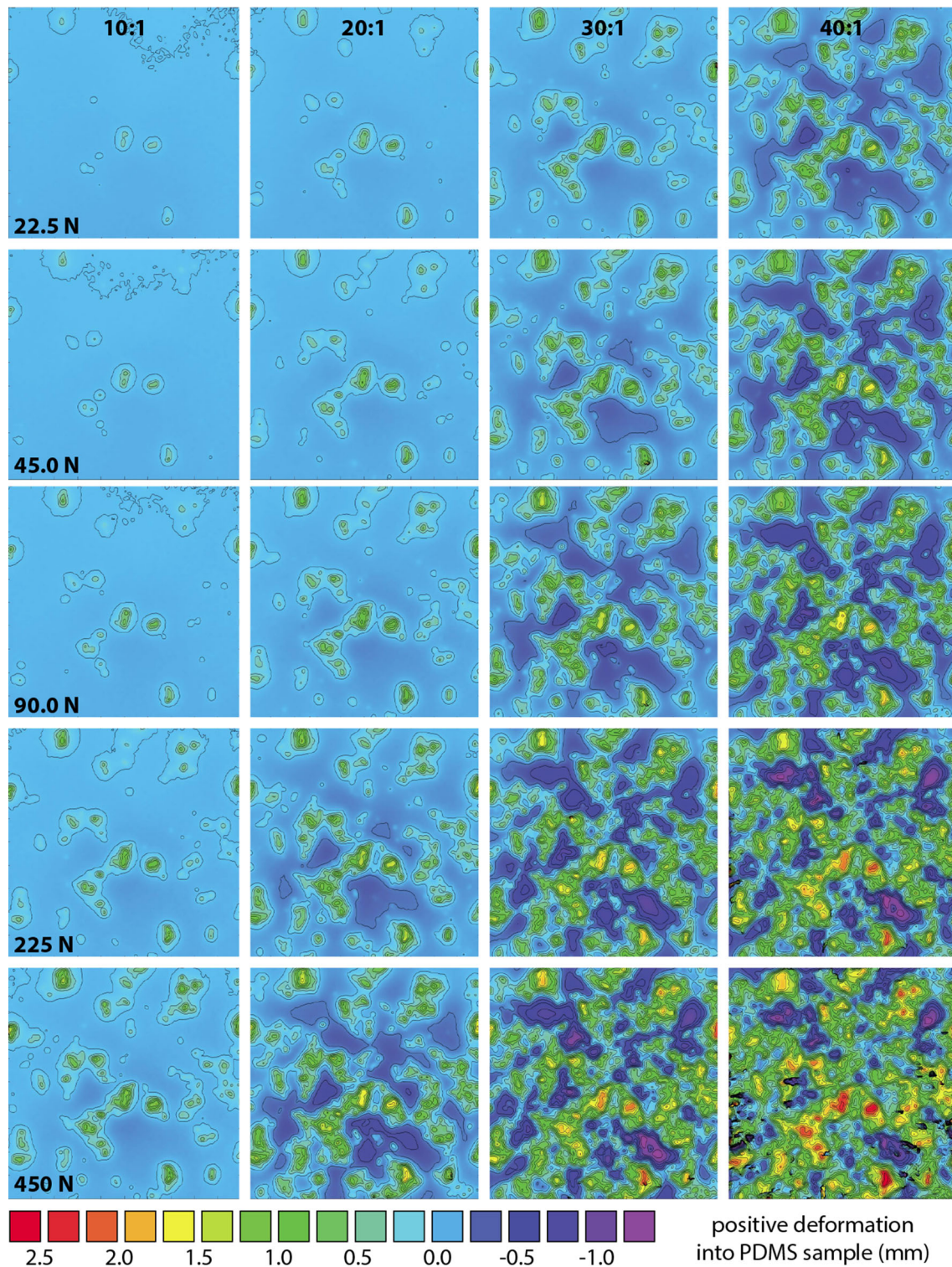


Fig. 2 Deformation maps for each PDMS sample at characteristic loads. The PDMS has both positive and negative deformations. The units associated with the deformation in the figure are all in

millimeters for these experiments. The topographic plots are for the entire apparent area of contact 100 mm × 100 mm

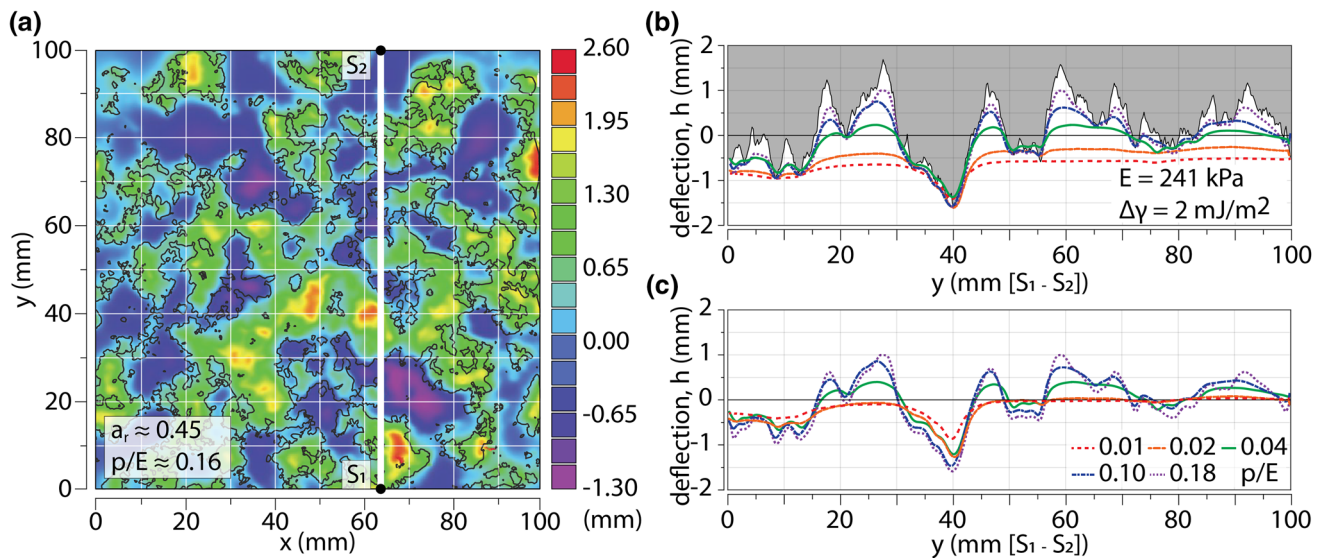


Fig. 3 Processed deformation map. **a** Contact area overlay from the FTIR method (*black lines*) overlaid with the DIC measurement of surface deformation. **b** Line scans depicting the deformation in the z -direction at $x = 63$ depicted as line $[S_1-S_2]$. Line scans represent the z -direction deformation at 22.5 N (0.01 p/E), 45.0 N (0.02 p/E),

112.5 N (0.04 p/E), 225 N (0.10 p/E), 450 N (0.18 p/E) for the 30:1 PDMS sample. Lines are shifted from absolute zero to show relative deformation at various reduced pressures. **c** Line scans as shown in **b** with z -direction deformations referenced from absolute zero

Each applied normal load was converted using Eq. (1) to a reduced pressure, \tilde{p} , which is equal to the nominal contact pressure, p , divided by the product of the composite modulus, E^* , and the surface root-mean-square gradient, \bar{g} . In this model, \bar{g} was equal to unity.

$$\tilde{p} = p / (E^* \bar{g}) \quad (1)$$

The elastic moduli of these samples were measured with a sphere-on-flat indentation experiment as discussed previously, and the composite moduli were entirely driven by the elastomer. A single line scan through the $x = 63$ mm position (S_1-S_2) is shown in Fig. 3b, and this line was selected because it passes through a range of high peaks and deep valleys in the surface topography. In Fig. 3b, the deformation of the PDMS surface is shown against the backdrop of the rough surface. In this representation, the rough surface is shown as the stationary feature, and as the load increases it is as if the PDMS is being pressed further into the rough surface. In this representation, the best reference point is the highest peak on the rough surface (located at roughly $Y = 0.4$, through which all of the lines pass and which represents the deepest penetration). This method of visualizing the surface deformation was found to be very useful during calibration, but is often confusing in terms of defining measurements of the surface deformation. With DIC, there is an absolute reference associated with the undeformed surface, which can be defined as zero deformation. As previously discussed, changes in the surface positions relative to this initial reference are given as surface deformation, and this is plotted for the same line

and loads in Fig. 3c. As discussed for the edge of contact, there are also significant regions of deformation up from the initial surface within the contact, and some of these regions are then involved in contacts that would not be predicted to occur from simple bearing area methods (this is one reason that the bearing area methods may under-predict contact areas as high relative pressure).

Both sealing [16, 17] and mixed lubrication [18–20] studies focus on regions on intimate contact and gaps within the contact. The gap height, as defined by Müser et al. [2], is a measure of the distance in the indenting direction between the indenting surface and the indented sample, and as defined by Carbone et al., it indicates the ability to conform to roughness of various intensities [21]. Unfortunately, gap height is not something that we can directly measure using the DIC method, as only the deformation of the contact surface is measured and the location of the indenting surface is not. However, for these experiments the surface profile is known (the surface itself is 3D printed), and by matching the profiles within contact the rough surface can be registered to the deformed surface (this is the method used to create Fig. 3b). As can be seen in Fig. 3b, the registration between the rough surface and the PDMS deformation remains a significant uncertainty contributor. For comparison to the simulation results from the “Contact Mechanics Challenge” [13], the surface gap at the mid-line ($X = 50$ mm following the convention defined in Fig. 3a) is plotted and compared as shown in Fig. 4a for a reduced pressure of 0.16. Despite all the difference between the simulation and experiment (scaled

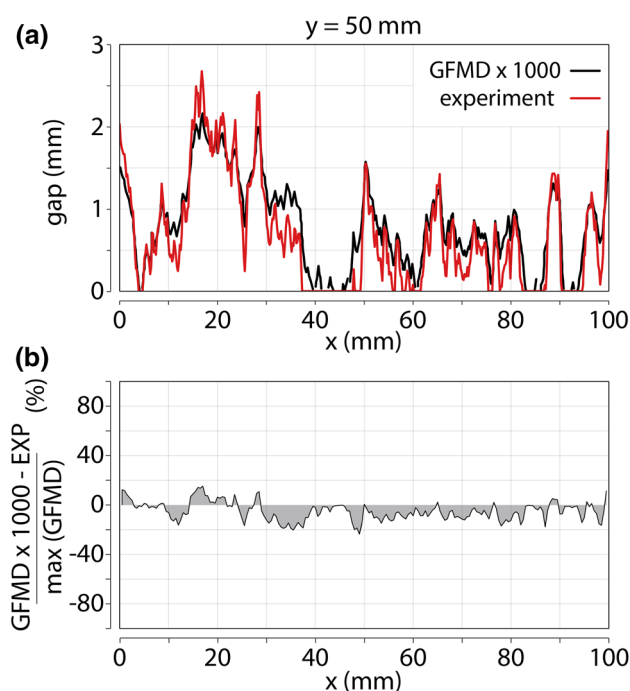


Fig. 4 **a** Digital image correlation (experiment) measurement of the gap compared to the gap computed through Green's function molecular dynamics for $x = 50$ mm and reduced pressure of 0.16. **b** The percent error between the Green's function molecular dynamics (GFMD) solution (which was considered the exact solution) [13] to the "Contact Mechanics Challenge" and the experimental results

1000 \times , non-periodic, low adhesion, and finite thickness), the agreement between them is within about 10% variation [13]. As shown in Fig. 4b, the errors (defined by the differences divided by the maximum gap) are within $\pm 10\%$. This result is undoubtedly somewhat fortuitous given all of the differences, but also extremely encouraging and promising for applications that need simulations of rough surface contact for prediction of performance, as in the case of seals and bearings.

4 Closing Remarks

The implementation of digital image correlation (DIC) to experimentally determine surface deformations under a scaled rough surface contact was shown to be a robust method of following the evolution deformation as a function of reduced pressure. These experiments were performed over a wide range of conditions, which was possible in part by a selection of four different PDMS substrate thicknesses. The production of a scaled model rough surface, which was 1000 \times larger than the model used in the "Contact Mechanics Challenge," was used in these experiments and compared favorably to the

predictions of gap within the surface contact ($\pm 10\%$). Together with the measurements of contact areas, these data provide a nearly complete description of the surface deformations for the randomly rough surface used in the "Contact Mechanics Challenge."

References

1. Tysoe, W.T., Spencer, N.D.: Contact-mechanics challenge. *Tribol. Lubr. Technol.* **71**, 96 (2015)
2. Müser, M.H., Dapp, W.B.: The contact mechanics challenge: problem definition. In: *Lehrstuhl für Material Simulation*. Word-Press (2015)
3. Bennett, A.I., Harris, K.L., Schulze, K.D., Uruëña, J.M., Pitenis, A.A., Müser, M.H., Angelini, T.E., Sawyer, W.G.: Contact area measurements of randomly rough surfaces. *Tribol. Lett.* (submitted) (2017)
4. McCormick, N., Lord, J.: Digital image correlation. *Mater. Today* **13**, 52–54 (2010). doi:10.1016/S1369-7021(10)70235-2
5. Yoneyama, S., Murasawa, G.: Digital image correlation, in experimental mechanics. In: *Encyclopedia of Life Support Systems (EOLSS)*. Developed under the Auspices of the UNESCO, Eolss Publishers, Paris, France (2009). <http://www.eolss.net>
6. Chu, T.C., Ranson, W.F., Sutton, M.A.: Applications of digital-image-correlation techniques to experimental mechanics. *Exp. Mech.* **25**, 232–244 (1985). doi:10.1007/BF02325092
7. Pan, B., Qian, K., Xie, H., Asundi, A.: Two-dimensional digital image correlation for in-plane displacement and strain measurement: a review. *Meas. Sci. Technol.* **20**, 62001 (2009). doi:10.1088/0957-0233/20/6/062001
8. Wu, P., Stanford, B., Bowman, W., Schwartz, A., Ifju, P.: Digital image correlation techniques for full-field displacement measurements of micro air vehicle flapping wings. *Exp. Tech.* **33**, 53–58 (2009). doi:10.1111/j.1747-1567.2008.00450.x
9. Hild, F., Roux, S.: Digital image correlation: from displacement measurement to identification of elastic properties—a review. *Strain* **42**, 69–80 (2006). doi:10.1111/j.1475-1305.2006.00258.x
10. Johnson, K.L., Kendall, K., Roberts, A.D.: Surface energy and the contact of elastic solids. *Proc. R. Soc. A Math. Phys. Eng. Sci.* **324**, 301–313 (1971). doi:10.1098/rspa.1971.0141
11. Style, R.W., Hyland, C., Boltyanskiy, R., Wettlaufer, J.S., Dufresne, E.R.: Surface tension and contact with soft elastic solids. *Nat. Commun.* (2013). doi:10.1038/ncomms3728
12. Style, R.W., Jagota, A., Hui, C.-Y., Dufresne, E.R.: Elastocapillarity: surface tension and the mechanics of soft solids. *Annu. Rev. Condens. Matter Phys.* **8**, 99–118 (2017). doi:10.1146/annurev-conmatphys-031016-025326
13. Müser, M.H., Dapp, W.B., Bugnicourt, R., Sainot, P., Lesaffre, N., Lubrecht, T.A., Persson, B.N.J., Harris, K.L., Bennett, A.I., Schulze, K.D., Rohde, S., Ifju, P., Sawyer, W.G., Angelini, T.E., Esfahani, H.A., Kadkhodaei, M., Akbarzadeh, S., Wu, J.J., Vorlaufer, G., Vernes, A., Solhjoo, S., Vakis, A.I., Jackson, R.L., Xu, Y., Streator, J., Rostami, A., Dini, D., Medina, S., Carbone, G., Bottiglione, F., Afferante, L., Monti, J., Pastewka, L., Robbins, M.O., Greenwood, J.A.: Meeting the contact-mechanics challenge. *Tribol. Lett.* (2017). doi:10.1007/s11249-017-0900-2
14. Lecompte, D., Smits, A., Bossuyt, S., Sol, H., Vantomme, J., Van Hemelrijck, D., Habraken, A.M.: Quality assessment of speckle patterns for digital image correlation. *Opt. Lasers Eng.* **44**, 1132–1145 (2006). doi:10.1016/j.optlaseng.2005.10.004
15. Johnson, K.L.: *Contact Mechanics*. Cambridge University Press, Cambridge (1985)

16. Dapp, W.B., Lücke, A., Persson, B.N.J., Müser, M.H.: Self-affine elastic contacts: percolation and leakage. *Phys. Rev. Lett.* **108**, 244301 (2012). doi:[10.1103/PhysRevLett.108.244301](https://doi.org/10.1103/PhysRevLett.108.244301)
17. Persson, B.N.J., Albohr, O., Tartaglino, U., Volokitin, A.I., Tosatti, E.: On the nature of surface roughness with application to contact mechanics, sealing, rubber friction and adhesion. *J. Phys. Condens. Matter* **17**, R1–R62 (2005). doi:[10.1088/0953-8984/17/1/R01](https://doi.org/10.1088/0953-8984/17/1/R01)
18. Krick, B.A., Vail, J.R., Persson, B.N.J., Sawyer, W.G.: Optical in situ micro tribometer for analysis of real contact area for contact mechanics, adhesion, and sliding experiments. *Tribol. Lett.* **45**, 185–194 (2012). doi:[10.1007/s11249-011-9870-y](https://doi.org/10.1007/s11249-011-9870-y)
19. Persson, B.N.J., Prodanov, N., Krick, B.A., Rodriguez, N., Mulakaluri, N., Sawyer, W.G., Mangiagalli, P.: Elastic contact mechanics: percolation of the contact area and fluid squeeze-out. *Eur. Phys. J. E* **35**, 5 (2012). doi:[10.1140/epje/i2012-12005-2](https://doi.org/10.1140/epje/i2012-12005-2)
20. Persson, B.N.J., Tartaglino, U., Albohr, O., Tosatti, E.: Rubber friction on wet and dry road surfaces: the sealing effect. *Phys. Rev. B* **71**, 35428 (2005). doi:[10.1103/PhysRevB.71.035428](https://doi.org/10.1103/PhysRevB.71.035428)
21. Carbone, G., Lorenz, B., Persson, B.N.J., Wohlers, A.: Contact mechanics and rubber friction for randomly rough surfaces with anisotropic statistical properties. *Eur. Phys. J. E* **29**, 275–284 (2009). doi:[10.1140/epje/i2009-10484-8](https://doi.org/10.1140/epje/i2009-10484-8)